

Spectroscopic characterization of nine binary star systems as well as HIP 107136 and HIP 107533 *

T. Heyne^{**}, M. Mugrauer, R. Bischoff, D. Wagner, S. Hoffmann, O. Lux, V. Munz, M. Geymeier, R. Neuhäuser

Astrophysikalisches Institut und Universitäts-Sternwarte Jena, Schillergäßchen 2-3, 07745 Jena, Germany

Received –, accepted –
Published online later

Key words binaries: spectroscopic, stars: individual: HIP 107162, HIP 23040, HIP 2225, HIP 30247, HIP 113048, HIP 25048, HIP 85829, HIP 77986, HIP 98194, HIP 107136, HIP 107533

We present the results of our 2nd radial velocity monitoring campaign, carried out with the Échelle spectrograph FLECHAS at the University Observatory Jena in the course of the Großschwabhausen binary survey between December 2016 and June 2018. The aim of this project is to obtain precise radial velocity measurements for spectroscopic binary stars in order to redetermine, verify, improve and constrain their Keplerian orbital solutions. In this paper we describe the observations, data reduction and analysis and present the results of this project. In total, we have taken 721 RV measurements of 11 stars and derived well determined orbital solutions for 9 systems (7 single-, and 2 double-lined spectroscopic binaries) with periods in the range between 2 and 70 days. In addition, we could rule out the orbital solutions for the previously classified spectroscopic binary systems HIP 107136 and HIP 107533, whose radial velocities are found to be constant on the km/s-level over a span of time of more than 500 days. In the case of HIP 2225 a significant change of its systematic velocity is detected between our individual observing epochs, indicating the presence of an additional companion, which is located on a wider orbit in this system.

© – WILEY-VCH Verlag GmbH & Co. KGaA, Weinheim

1 Introduction

The University Observatory Jena is located close to the village Großschwabhausen roughly 10 km west of the city Jena (Pfau 1984). Since 2013 the fibre-linked Échelle spectrograph FLECHAS (Mugrauer et al. 2014) is mounted at the 90-cm reflector telescope while it is operated in the Nasmyth mode ($D = 90$ cm, $f/D = 15$). As part of the Großschwabhausen binary survey (Mugrauer et al. 2016) a radial velocity (RV) monitoring program was started in 2015 (Bischoff et al. 2017) in order to redetermine, verify, improve and constrain the Keplerian orbital solutions of spectroscopic binaries, selected from the 9th Catalogue of Spectroscopic Binary Orbits (SB9 hereafter, see Pourbaix et al. 2004). The SB9 yields information about orbital elements of several thousand spectroscopic binary systems. The binaries are ranked by different orbit grades with values from 0 (poor) to 5 (definitive), dependant on the quality of their orbital solutions.

The project presented here is a continuation of this RV monitoring program with a target sample, chosen from the SB9, with less constrained orbital solutions, which exhibit

orbital grades of 3 or lower. The properties of the selected targets are summarized in Tab. 1. Section 2 of this paper describes in detail the spectroscopic observations, taken in this project, and the data reduction. Section 3 provides information about the procedure of measuring individual radial velocities. The derived Keplerian orbital solutions are presented in the Section 4 and their properties are discussed in the last section of this paper.

2 Observations and data reduction

In the course of our RV monitoring project 11 targets were observed during two observing epochs between December 2016 and May 2017, and from January to June 2018. In total, more than 33 spectra could be taken for each target with FLECHAS in its 1x1 binning mode, which provides a spectral resolving power of $R \sim 9300$. On average, the obtained spectra of all targets exhibit a signal-to-noise-ratio (SNR) in the range between about 110 and 300 (as measured at a wavelength of 6500 Å), which is adequately high to obtain accurate RV measurements. In general three spectra, each with a minimum integration time of 150 s were taken for each target to remove cosmics from the resulting spectra, and to achieve a sufficiently high SNR . Directly before the spectroscopy of each target 3 flat-field frames of a tungsten lamp with an exposure time of 5 s were taken followed by 3 spectra of a ThAr lamp (with more than 700 detected emission lines) for wavelength calibration.

* Based on observations obtained with telescopes of the University Observatory Jena, which is operated by the Astrophysical Institute of the Friedrich-Schiller University.

** Corresponding author: T. Heyne, Astrophysikalisches Institut und Universitäts-Sternwarte Jena, Schillergäßchen 2-3, 07745 Jena, Germany. e-mail: therese.heyne@uni-jena.de

Table 1 Properties of the observed targets. For all targets their equatorial coordinates (RA, Dec), V-band magnitude (V) and spectral type (SpT) are given together with their orbital solution (period P , periastron time T_0 , eccentricity e , argument of periastron ω , RV semi-amplitude K , and systematic velocity γ) as listed in the SB9 with an orbit grade of 3 or lower.

Target	RA _{J2000} [hh mm ss.ss]	Dec _{J2000} [dd mm ss.s]	V [mag]	SpT	Grade	P [d]	T_0 [JD]	e	ω [°]	K [km/s]	γ [km/s]	Ref.
HIP 107162	21 42 22.96	+41 04 37.3	5.74	A0V	2	1.729	2424255.8	0.0	0.0	110*	-25.5	[a]
HIP 23040	04 57 17.20	+53 45 07.6	4.43	A1V	3	3.8845	2418686.7	0.0	0.0	35.8	-9.5	[b]
HIP 2225	00 28 13.65	+44 23 40.0	5.20	A2Vs	3	3.9558	2418841.6	0.15	233.2	41.7	+2.0	[c]
HIP 30247	06 21 46.13	+53 27 07.8	5.36	F5III	3	6.5013	2423634.2	0.02	330.6	31.7	-1.5	[d]
HIP 113048	22 53 40.16	+44 44 57.0	5.81	A3m	1	24.1635	2440000.4	0.2	5.0	10.1	+6.7	[e]
HIP 25048	05 21 48.42	+41 48 16.5	5.22	B5V	1	35.5	2430000.0	0.0	0.0	28.0	+19.0	[f]
HIP 85829	17 32 16.03	+55 10 22.6	4.89	A4m	2	38.128	2440022.4	0.04	0.6	9.8	-16.7	[e]
HIP 77986	15 55 30.59	+42 33 58.3	5.75	B7IV-Ve	1	46.194	2441473.8	0.34	5.0	12.0	-19.3	[g]
HIP 98194	19 57 13.87	+40 22 04.2	5.41	B5Vp	2	70.22	2439762.1	0.34	302	41.4	-20.1	[h]
HIP 107136	21 42 05.67	+51 11 22.6	4.67	B3V	1	26.33	2431306.5	0.0	0.0	16.5	-8.2	[i]
HIP 107533	21 46 47.61	+49 18 34.5	4.24	B3III	2	72.0162	2428410.6	0.34	238.1	7.8	-12.3	[j]

* Amplitude of both components of this double-lined spectroscopic binary system.

References for the listed orbital solutions from the SB9:

[a] Luyten 1936	[b] Lucy et al. 1971	[c] Udick 1912	[d] Harper 1925	[e] Abt et al. 1985
[f] Blaauw et al. 1963	[g] Heard et al. 1975	[h] Batten et al. 1982	[i] Fehrenbach 1948	[j] Taffara 1939

In addition, dark frames for all used exposure times were taken in each observing night for the dark current removal. The complete spectroscopic data reduction was done with the FLECHAS software pipeline, developed at the Astrophysical Institute Jena, which is optimized for the reduction of FLECHAS data. The software includes dark current subtraction, flat-fielding, extraction and wavelength calibration of the individual spectral orders, as well as the averaging and normalization of all spectroscopic data (Mugrauer et al. 2014). Throughout this project, 2163 spectra of all targets could be taken, which results in 721 fully reduced spectra with a total integration time of 132 h. The details of the observations of all targets are summarized in the observation log, which is listed in Tab. 2.

Table 2 Observation log. For each target we list the number of observations (N_{Obs}), the dates of the first and last successful observation, as well as the average signal-to-noise ratio ($< SNR >$) of all spectra, as measured at $\lambda = 6500 \text{ \AA}$.

Target	N_{Obs}	first obs.	last obs.	$< SNR >$
HIP 107162	53	2016 Dec 5	2018 Jun 3	117
HIP 23040	104	2016 Dec 6	2018 May 25	167
HIP 2225	36	2016 Dec 6	2018 Jun 3	122
HIP 30247	111	2016 Dec 6	2018 May 28	134
HIP 113048	42	2016 Dec 5	2018 Jun 3	119
HIP 25048	69	2016 Dec 5	2018 May 1	114
HIP 85829	77	2016 Dec 5	2018 Jun 3	162
HIP 77986	63	2016 Dec 5	2018 Jun 3	117
HIP 98194	59	2016 Dec 5	2018 Jun 3	147
HIP 107136	55	2016 Dec 5	2018 Jun 3	141
HIP 107533	52	2016 Dec 5	2018 Jun 3	193

3 Radial velocity measurements

The RVs of the targets are determined for all observing dates in the fully reduced spectra of the stars, by measuring the wavelengths of the first three Hydrogen Balmer lines (H_{α} : $\lambda_0 = 6562.81 \text{ \AA}$, H_{β} : $\lambda_0 = 4861.34 \text{ \AA}$, H_{γ} : $\lambda_0 = 4340.48 \text{ \AA}$), which are prominent lines in the spectra of early type stars with spectral type B to F. Thereby, the wavelength of the spectral lines are determined by fitting a Gaussian profile on the Doppler broadening dominated line cores, using the IRAF standard script SPLIT. The RV of the stars is derived from the measured Doppler shifts ($\lambda - \lambda_0$) of the individual spectral lines by

$$RV = c \cdot \frac{\lambda - \lambda_0}{\lambda_0} + BC \quad (1)$$

with c the speed of light, and BC the barycentric correction.

In the fully reduced spectra the RVs of all stars, obtained by the core fitting of their Balmer lines, are averaged and their standard deviation is determined. This yields for all observing dates the RV of each target, including its uncertainty.

In addition, telluric spectral lines, detected in the different spectral orders are used to check the stability of the wavelength calibration of FLECHAS throughout our RV monitoring project. The RVs of the measured telluric lines scatter on average on the 0.9 km s^{-1} level, which is consistent with the reached RV precision of the different observed targets. The long-term RV stability of the spectrograph was already verified by Irrgang et al. 2016 and Bischoff et al. 2017, and is also confirmed by our measurements, taken in the course of this project.

While most of the observed targets are classified as single-lined spectroscopic binaries, a splitting of the spec-

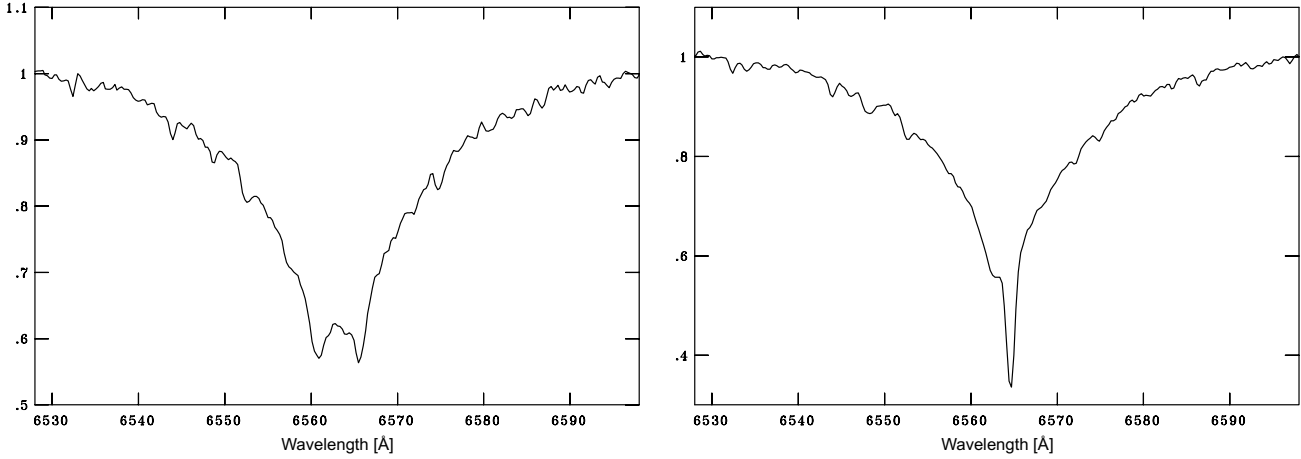


Fig. 1 The H_{α} -line profile of HIP 107162 (left) and HIP 2225 (right), extracted from the FLECHAS spectra of the stars taken on 2016 Dec 21. The SB2 nature of both stars is clearly detected. While the spectral lines of the individual components of HIP 107162 are resolved in the FLECHAS spectra, taken at orbital phases with maximal RV deviations from the systematic velocity, the lines of the components of HIP 2225 remain significantly blended at all orbital phases.

tral lines is detected in some spectra of HIP 107162, and HIP 2225, as it is illustrated in Fig. 1. Hence, these stars are double-lined spectroscopic binaries, in which the RVs of their components can be measured separately.

In order to obtain the wavelengths of the blended spectral lines of the observed SB2s the line-deblending task in SPLLOT is used if applicable. In the case of HIP 107162 the wavelengths of the spectral lines are determined using line-deblending at orbital phases with maximal RV deviations from the systematic velocity. In contrast for HIP 2225 the spectral lines of the individual components remain significantly blended even at extreme orbital phases, and the line-deblending fails to provide the wavelengths of both components, only the wavelength of the spectral lines of the primary star can be measured. In order to determine the wavelengths of the spectral lines of the secondary component we flip all normalized spectra at the line centers of the primary and subtract them from the original spectra. As illustrated in Fig. 2, in these difference spectra the line profile of the primary component is well removed and only the spectral line of the secondary component remains (as a positive/negative pair), whose wavelength is determined by Gaussian fitting.

The determined RVs of our targets with their uncertainties are summarized for all observing dates (given as barycentric Julian date BJD) in Tab. A1 to A11. The reached RV precision ranges between 0.6 and 2.8 km/s for the single-lined, and between 2.3 and 20.4 km/s for the double-lined spectroscopic binaries, respectively.

4 Orbit determination

The RV variation of a component of a binary star due to Keplerian orbital motion around the barycenter of the stellar system is described by

$$RV = K \cdot [e \cdot \cos(\omega) + \cos(\omega + \nu)] + \gamma \quad (2)$$

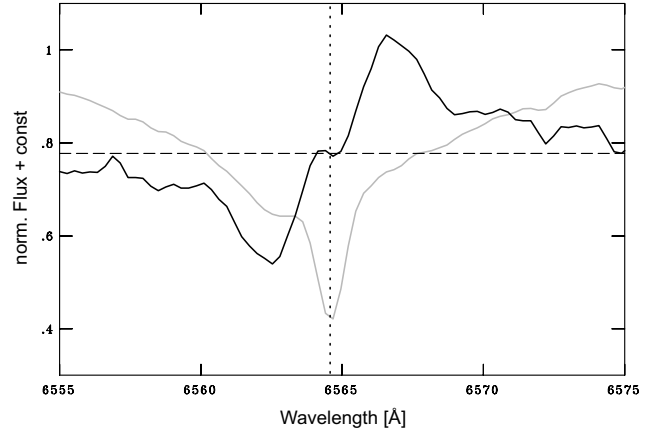


Fig. 2 Detail view of the H_{α} line-profile (grey line, with its center indicated with a dotted vertical line) of HIP 2225, extracted from the normalized FLECHAS spectrum of the star, taken on 2016 Dec 21. The difference spectrum, in which the spectral line of the primary component is subtracted, is illustrated as dark line with its zero normalized flux level, indicated as dashed line. The spectral line of the fainter secondary component clearly appears as positive/negative pair in the difference spectrum.

where K is the semi-amplitude, ν the true anomaly of the component, ω the argument of periastron, e the eccentricity of its orbit and γ the systematic velocity of the stellar system.

The semi-amplitude

$$K = \frac{2\pi \cdot a \sin(i)}{P \cdot \sqrt{1 - e^2}} \quad (3)$$

depends on the minimum semi-major axis $a \sin(i)$, the orbital period P , and the orbital eccentricity of the component of the spectroscopic binary system.

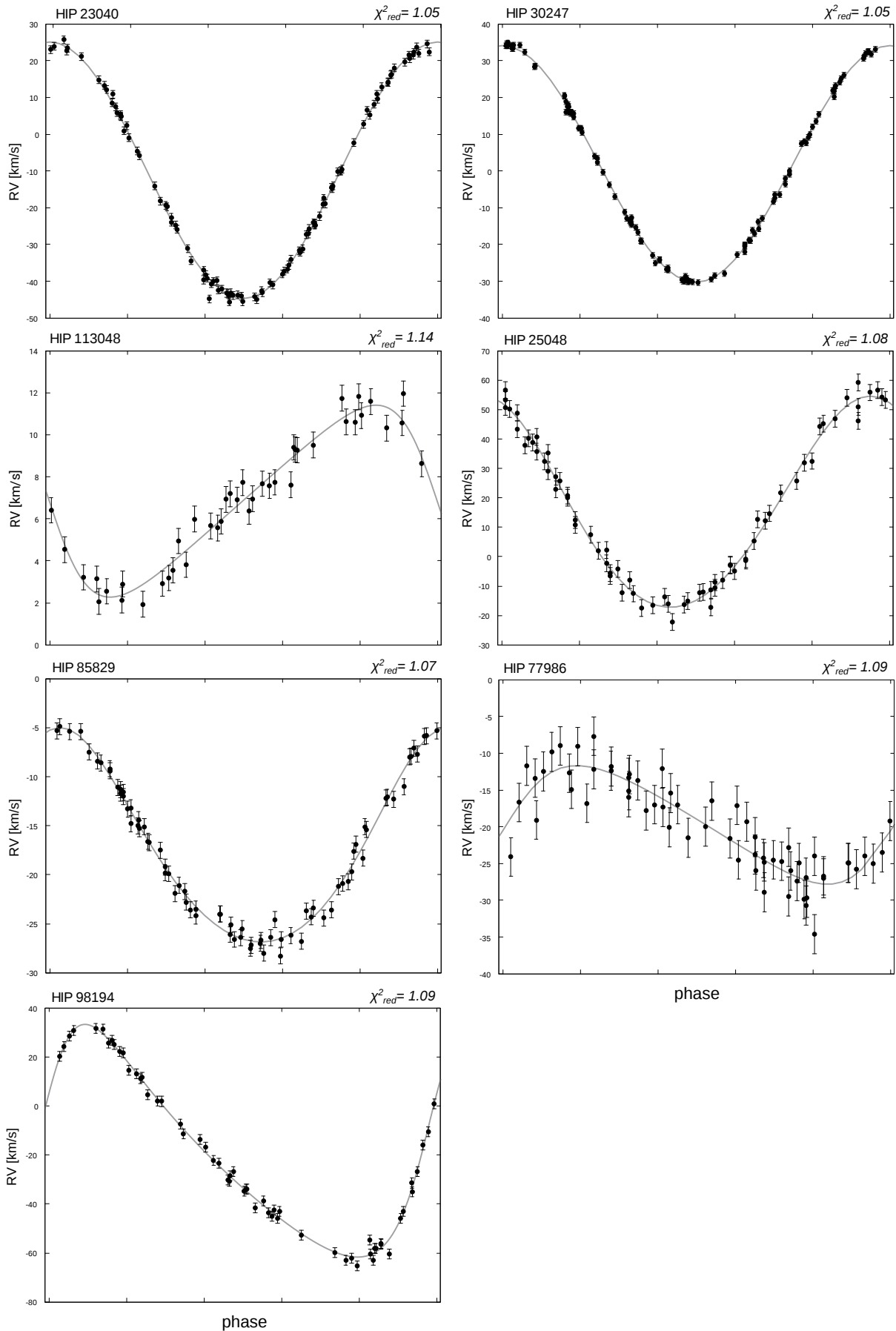
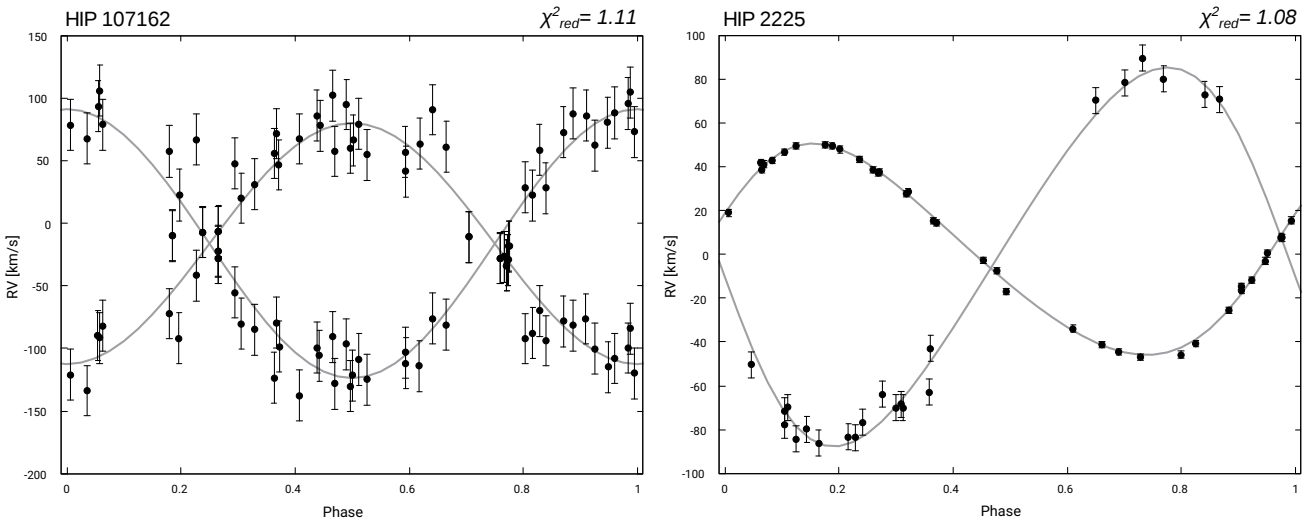


Fig. 3 The phase-folded RV curves of the 7 single-lined spectroscopic binaries, observed in the course of our project. For all targets their RV measurements are shown with their uncertainties together with the derived best fitting Keplerian orbital solutions (grey lines).

Table 3 The derived Keplerian orbital elements with their uncertainties of all spectroscopic binaries, observed in this project.

Target	P [d]	T [BJD]	e	ω [°]	K [km/s]	γ [km/s]
HIP 107162 A	1.728 ± 0.061	2457726.95 ± 0.01	0 [fixed]	180 [fixed]	96.2 ± 3.9	-16.3 ± 2.0
HIP 107162 B	1.728 ± 0.061	2457726.95 ± 0.01	0 [fixed]	0 [fixed]	107.4 ± 3.9	-16.3 ± 2.0
HIP 23040	3.884 ± 0.001	2457726.05 ± 0.01	0 [fixed]	0 [fixed]	34.9 ± 0.2	-9.8 ± 0.1
HIP 2225 A	3.956 ± 0.001	2457727.19 ± 0.06	0.136 ± 0.011	276.0 ± 5.4	48.4 ± 1.0	0 [fixed]
HIP 2225 B	3.956 ± 0.001	2457727.19 ± 0.06	0.136 ± 0.011	96.0 ± 5.4	86.5 ± 1.0	0 [fixed]
HIP 30247	6.501 ± 0.001	2457726.71 ± 0.01	0 [fixed]	0 [fixed]	32.2 ± 0.1	$+1.9 \pm 0.1$
HIP 113048	24.190 ± 0.022	2457724.80 ± 0.40	0.296 ± 0.035	90.6 ± 8.9	4.6 ± 0.2	$+6.9 \pm 0.1$
HIP 25048	34.507 ± 0.013	2457725.50 ± 1.00	0.073 ± 0.014	20.5 ± 10.9	35.9 ± 0.5	$+16.2 \pm 0.4$
HIP 85829	38.058 ± 0.013	2457714.88 ± 0.66	0.128 ± 0.012	347.4 ± 6.1	10.9 ± 0.1	-17.3 ± 0.1
HIP 77986	45.862 ± 0.108	2457723.93 ± 2.26	0.234 ± 0.059	264.4 ± 18.6	8.1 ± 0.5	-19.6 ± 0.3
HIP 98194	70.219 ± 0.031	2457670.27 ± 0.31	0.351 ± 0.008	293.9 ± 1.5	47.5 ± 0.4	-21.0 ± 0.3

**Fig. 4** The phase-folded RV curves of the double-lined spectroscopic binaries HIP 107162, and HIP 2225. The RV measurements are shown with their uncertainties together with the derived best fitting Keplerian orbital solutions (grey lines).

For all spectroscopic binaries the orbital elements together with their uncertainties are determined by fitting Keplerian orbital solutions on the obtained RV measurements of the systems, using the spectroscopic binary solver (Johnson 2004). The derived orbital solutions are illustrated as grey lines in the phase-folded RV curves in Fig. 3, and their orbital elements are summarized in Tab. 3. The orbital solutions all exhibit reduced chi-squared values of $\chi_{red}^2 \sim 1$ and their semi-amplitudes are at least three times larger than the given RV uncertainties, i.e. the FLECHAS spectroscopy significantly detects the Keplerian motion of all binary systems, monitored in this project.

For HIP 30247 ($e = 0.004 \pm 0.003$), HIP 23040 ($e = 0.000 \pm 0.006$) and HIP 107162 ($e = 0.012 \pm 0.035$) the derived orbital solutions are consistent with circular orbits. Therefore, for these particular systems the orbit fitting was repeated, whereby the eccentricity was fixed to $e = 0$.

In order to check the stability of the determined orbital solutions over the whole span of time, covered by our RV monitoring project, at first we derived the orbital

solutions of all systems for both observing epochs separately. For the majority of all systems, these orbital solutions agree with each other within their uncertainties. Hence, for these systems we use all available RV data of both observing epochs to determine the best fitting Keplerian orbital solution. In contrast, for HIP 2225 a significant difference in its systematic velocity is detected between the first ($\gamma = 22.6 \pm 0.4$ km/s) and second ($\gamma = 13.1 \pm 0.4$ km/s) observing epoch. In order to determine an orbital solution for this particular system, based on all RV data, in each observing epoch the derived systematic velocity is subtracted from the RV measurements, resulting in a fixed systematic velocity ($\gamma = 0$ km/s) in the final orbital solution of HIP 2225.

For HIP 107136 and HIP 107533 no significant RV variation could be detected. Both stars exhibit a constant RV of -5.8 ± 3.1 km/s, and -17.2 ± 1.2 km/s, respectively.

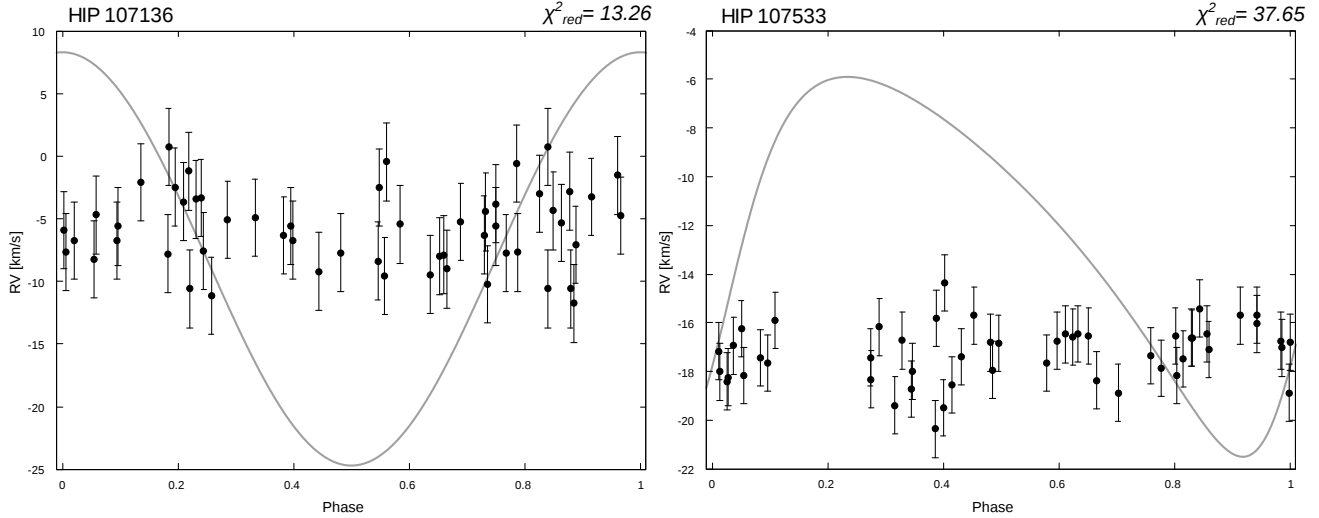


Fig. 5 RV measurements of HIP 107136 and HIP 107533, taken in the course of our spectroscopic monitoring program with FLECHAS, phase-folded with the orbital period of the stars, as given in the SB9. The orbital solutions from the SB9 are shown as grey lines, which are clearly inconsistent ($\chi_{red}^2 > 13$) with the RV data of both stars, taken in this project.

5 Discussion

In the course of our RV monitoring project more than 30 RV measurements could be recorded with FLECHAS for all targets, yielding homogeneously covered phase-folded RV curves of all observed spectroscopic binary systems. For the majority of these systems our RV data verify and constrain the given orbital solutions, which are listed in the SB9, and are summarized in Tab. 1.

For HIP 25048 the relative difference between the orbital period, obtained in this project, and the one listed in the SB9 is 2.9 % and thus significantly larger than for the remaining 9 spectroscopic binaries, among which HIP 77986 exhibits the largest difference of only 0.7 %. The eccentricity of this system deviates by 0.11 and its argument of periastron by more than 100° from the SB9 value, which corresponds to the largest difference of both quantities, found among all targets, investigated in this project.

In general, the semi-amplitudes of all systems, derived here, deviate by more than 10 % from the amplitudes, given in the SB9. In the case of HIP 113048 the semi-amplitude, listed in the SB9, is even twice as large as the amplitude of the system derived from our RV measurements. Only for HIP 30247 and HIP 23040 the obtained semi-amplitudes agree on the 3 percent level with the SB9 amplitudes.

On average, the systematic velocities of all systems, derived in this project, differ by about 2 km/s from the velocities given in the SB9, with the largest difference of about 9 km/s found for HIP 107162.

HIP 107136, and HIP 107533 are both listed as single-lined spectroscopic binaries in the SB9 but no significant RV variation could be detected for these stars in our RV monitoring project within a span of time of 545 days. Furthermore, as illustrated in Fig. 5, our RV measurements clearly rule out the orbital solutions of both stars, as given

in the SB9, but prove that they exhibit constant RVs of -5.8 ± 3.1 km/s, and -17.2 ± 1.2 km/s, respectively.

HIP 2225, which is classified as a single-lined spectroscopic binary in the SB9, turns out to be a actually a double-lined spectroscopic binary system, as confirmed with the RV measurements, taken in the course of our project. Furthermore, while for the majority of the observed binary stars their orbital solutions, derived for both observing epochs separately, are consistent with each other within their uncertainties, HIP 2225 exhibits a significant variation of its systematic velocity $\Delta\gamma = -9.5 \pm 0.6$ km/s between both observing epochs, which yields $\dot{\gamma} = -7.8 \pm 1.4$ km s $^{-1}$ yr $^{-1}$. This deviation of the systematic velocity indicates the presence of a further companion on a wider orbit in this system. For a companion on circular orbit with the radius a one expects a maximal deviation of the systematic velocity

$$\dot{\gamma}_{max} = MG/a^2 \quad (4)$$

with M the total mass of the system.

Indeed, Horch et al. 2015 detected a faint companion-candidate ($\Delta m \sim 2.4$ mag) in the (infra)red spectral range, which is located only about 0.1 arcsec southwest of HIP 2225. If this candidate is a bound companion of the star its mass can be approximated using its magnitude difference to HIP 2225, as well as the spectral type of the star (A2V, as given in the SB9). According to the spectral type - effective temperature relation from Pecaute et al. 2013 this yields a mass of the companion-candidate of about $1.1 M_\odot$. With the mass of HIP 2225 ($2.26 M_\odot$, as determined by Allende Prieto et al. 1999) and the derived mass-ratio of the spectroscopic binary (~ 0.56 , see Tab. 5), the total mass of the HIP 2225 system can be estimated to be $4.6 M_\odot$.

Hence, assuming $\dot{\gamma} = \dot{\gamma}_{max}$, the orbital radius of the wide companion is about 10.5 au, which corresponds to an orbital period of ~ 16 yr. At the distance of HIP 2225

($\pi = 11.2634$ mas, Gaia Collaboration et al. 2018) this yields a maximal projected angular separation between the companion and the star of about 0.12 arcsec, fully consistent with the observed angular separation of the companion-candidate, directly imaged by Horch et al. 2015. Therefore, we consider this candidate as a bound companion of HIP 2225, which induces the detected deviation of the systematic velocity of this system. Furthermore, the observed higher eccentricity of the close spectroscopic binary might also indicate the presence of an additional companion of HIP 2225. In order to further constrain the orbital parameters of this wide companion, which should be denoted as HIP 2225 C, additional RV monitoring and high contrast imaging observations are needed, which have to be carried out within the next one and a half decades.

Finally, for all observed single-lined spectroscopic binaries their mass-function $f(M)$ and the minimum semi-major axis $a \sin(i)$ can be derived from the determined orbital elements of these systems

$$f(M) = \frac{(1 - e^2)^{\frac{3}{2}} \cdot P \cdot K^3}{2\pi \cdot G} \quad (5)$$

$$a \sin(i) = \frac{K \cdot P \cdot \sqrt{1 - e^2}}{2\pi} \quad (6)$$

which are listed with their uncertainties in Tab. 4.

Table 4 The derived mass function $f(M)$ and minimum semi-major axis $a \sin(i)$ of all single-lined spectroscopic binary systems, observed in this project.

Target	$f(M)$ [M_{\odot}]	$a \sin(i)$ [au]
HIP 23040	0.0171 ± 0.0002	0.0125 ± 0.0001
HIP 30247	0.0224 ± 0.0002	0.0192 ± 0.0001
HIP 113048	0.00021 ± 0.00002	0.0097 ± 0.0004
HIP 25048	0.1644 ± 0.0069	0.1136 ± 0.0016
HIP 85829	0.0050 ± 0.0002	0.0379 ± 0.0005
HIP 77986	0.0023 ± 0.0005	0.0331 ± 0.0022
HIP 98194	0.6392 ± 0.0186	0.2869 ± 0.0028

In addition, for the double-lined spectroscopic binaries the minimum-masses of their components

$$M_{1/2} \sin^3(i) = \frac{(1 - e^2)^{3/2} P}{2\pi G} K_{2/1} (K_1 + K_2)^2 \quad (7)$$

as well as their minimum semi-major axes can be determined, which are summarized with their uncertainties in Tab. 5.

The single-lined spectroscopic binaries exhibit mass-functions in the range between 0.0002 and $0.64 M_{\odot}$ and their minimum semi-major axes range between about 0.01 and 0.29 au.

While the double-lined spectroscopic binary HIP 107162 consists of two comparably massive stars

Table 5 Derived minimum-masses $M \sin^3(i)$ and semi-major axes $a \sin(i)$ for both components of the observed double-lined spectroscopic binary systems HIP 107162, and HIP 2225.

Target Component	$M \sin^3(i)$ [M_{\odot}]	$a \sin(i)$ [au]
HIP 107162 A	0.798 ± 0.001	0.0153 ± 0.0003
HIP 107162 B	0.715 ± 0.001	0.0171 ± 0.0003
HIP 2225 A	0.628 ± 0.016	0.0176 ± 0.0006
HIP 2225 B	0.354 ± 0.016	0.0311 ± 0.0006

on circular orbits (consistent with the result, given in the SB9), the components of HIP 2225 exhibit a mass-ratio of 0.56 ± 0.03 , and revolve around their barycenter on close ($a < 0.1$ au) and slightly eccentric ($e \sim 0.14$) orbits with a period of about 4 days. In addition, a further companion, HIP 2225 C, could spectroscopically be identified in this system, which orbits the close binary with a period of about 16 yr, or more.

The RV monitoring project of spectroscopic binaries, presented here, is part of an ongoing program, carried out at the University Observatory Jena. In the future we will continue to take RV measurements of the remaining targets of this program until precise orbital solutions for these systems can be derived from our RV data. These RV measurements and orbital solutions, together with those presented in this paper, will be made available online at VizieR (Ochsenbein, Bauer & Marcout 2000).

Acknowledgements. We thank all observers, who have been involved in some of the observations of this project at the University Observatory Jena, in particular H. Gilbert, T. Zehe, A. Trepanovski, and F. Schiefeneder. This publication makes use of data products of the VizieR databases, as well as SIMBAD, both operated at CDS, Strasbourg, France.

References

- Abt, H. A., & Levy, S. G. 1985, ApJS, 59, 229
 Allende Prieto C., Lambert D. L. 1999, A&A, 352, 555
 Batten, A. H., Fisher, W. A. & Fletcher, J. M. 1982, PASP, 94, 515
 Bischoff, R., Mugrauer, M. Zehe, T. et al. 2017, AN, 338, 671
 Blaauw, A. & van Albada, T. S. 1963, ApJ, 137, 791
 Dworetzky, M. M., 1983, MNRAS, 203, 917
 Fehrenbach, C. 1948, AnAp, 11, 157
 Gaia Collaboration, et al., 2018, A&A, 616, A1
 Harper, W. E. 1925, PDAO, 3, 189
 Horch, E. P. et al. 2015, AJ, 150, 151
 Heard, J. F., Hurkens, R. & Harmanec, P. 1975, A&A, 42, 47
 Irrgang, A., Desphande, A. & Moehler, S. 2016, A&A, 591, 6
 Johnson, D. O. 2004, JAD, 10, 3
 Lucy, L. B., & Sweeney, M. A. 1971, AJ, 76, 544
 Luyten, W. J. 1936, ApJ, 84, 85
 Mugrauer, M., Avila, G. & Guirao, C. 2014, AN, 335, 417
 Mugrauer, M., Buder, S., Reum, F. et al. 2016, AN, 337, 226
 Ochsenbein F., Bauer P., Marcout J., 2000, A&AS, 143, 23
 Pecaut M. J. & Mamajek E. E. 2013, ApJS, 208, 9

Pfau, W. 1984, *JenRu*, 29, 121
 Pourbaix, D. et al. 2004, *A&A*, 424, 727
 Stickland, D. J. 1987, *Obs*, 12, 5
 Taffara, S. 1939, *MmSAI*, 12, 279
 Udick, S. 1912, *PAIO*, 2, 191
 Zehe, T., Mugrauer, M., Neuhauser, R. et al. 2018, *AN*, 339, 46

A Radial velocity measurements

Table A1 RV measurements of HIP 107162

Date of Obs. BJD – 2450000	RV ₁ [km/s]	RV ₂ [km/s]
7728.27661	-26.8 ± 20.2	-26.8 ± 20.4
7729.20791	+20.2 ± 20.2	-80.1 ± 20.4
7743.26094	+86.1 ± 20.2	-99.3 ± 20.4
7744.20421	-99.6 ± 20.2	+95.7 ± 20.4
7760.24442	-22.4 ± 20.2	-22.4 ± 20.4
7764.27020	+41.5 ± 20.2	-111.8 ± 20.4
7773.22328	-18.3 ± 20.2	-18.3 ± 20.4
7775.25176	-114.8 ± 20.2	+80.5 ± 20.4
7775.33198	-119.9 ± 20.2	+73.1 ± 20.4
7776.22491	+79.2 ± 20.2	-108.8 ± 20.4
7780.22873	-69.9 ± 20.2	+58.6 ± 20.4
7782.23129	-84.1 ± 20.2	+104.8 ± 20.4
7782.71285	-06.4 ± 20.2	-06.4 ± 20.4
7798.26671	-27.9 ± 20.2	-27.9 ± 20.4
7800.24044	+67.5 ± 20.2	-137.7 ± 20.4
7840.59677	-28.0 ± 20.2	-28.0 ± 20.4
7843.60805	+66.4 ± 20.2	-121.6 ± 20.4
7874.49172	+46.8 ± 20.2	-98.4 ± 20.4
7880.48457	-93.9 ± 20.2	+28.2 ± 20.4
8151.17594	+57.3 ± 20.2	-128.0 ± 20.4
8151.22274	+59.9 ± 20.2	-130.0 ± 20.4
8151.27354	+54.8 ± 20.2	-124.9 ± 20.4
8155.23215	-87.8 ± 20.2	+22.2 ± 20.4
8172.63542	-81.7 ± 20.2	+87.7 ± 20.4
8173.63656	+102.1 ± 20.2	-90.7 ± 20.4
8174.65402	-89.8 ± 20.2	+93.4 ± 20.4
8178.65121	+71.5 ± 20.2	-79.6 ± 20.4
8197.59560	+31.2 ± 20.2	-84.8 ± 20.4
8202.53067	-09.9 ± 20.2	-09.9 ± 20.4
8207.50535	-81.9 ± 20.2	+78.7 ± 20.4
8215.52609	-11.0 ± 20.2	-11.0 ± 20.4
8216.54567	+47.9 ± 20.2	-55.2 ± 20.4
8217.54034	-78.3 ± 20.2	+72.6 ± 20.4
8218.53161	+78.0 ± 20.2	-105.6 ± 20.4
8219.50427	-120.9 ± 20.2	+78.4 ± 20.4
8220.51770	+56.9 ± 20.2	-103.0 ± 20.4
8228.52748	-41.8 ± 20.2	+66.9 ± 20.4
8229.52273	-92.0 ± 20.2	+28.8 ± 20.4
8230.49063	+55.6 ± 20.2	-123.4 ± 20.4
8238.43508	-108.1 ± 20.2	+88.2 ± 20.4
8240.54190	-72.1 ± 20.2	+57.4 ± 20.4
8243.53264	-76.4 ± 20.2	+86.1 ± 20.4
8244.53565	+94.9 ± 20.2	-96.5 ± 20.4
8245.51672	-91.6 ± 20.2	+106.0 ± 20.4
8246.52495	+90.8 ± 20.2	-76.0 ± 20.4

Continued		
Date of Obs. BJD – 2450000	RV ₁ [km/s]	RV ₂ [km/s]
8259.58250	–91.8 ± 20.2	+22.6 ± 20.4
8260.57475	–33.6 ± 20.2	–33.6 ± 20.4
8264.48912	–133.6 ± 20.2	+67.6 ± 20.4
8265.49587	+63.7 ± 20.2	–114.0 ± 20.4
8267.49156	–29.4 ± 20.2	–29.4 ± 20.4
8269.48234	–100.3 ± 20.2	+62.3 ± 20.4
8272.48952	+61.0 ± 20.2	–81.2 ± 20.4
8273.47945	–07.3 ± 20.2	–07.3 ± 20.4

Continued	
Date of Obs. BJD – 2450000	RV [km/s]
8146.28347	+5.0 ± 1.1
8149.35755	+24.6 ± 1.1
8151.38000	–44.0 ± 1.1
8151.59191	–43.1 ± 1.1
8154.45375	–18.2 ± 1.1
8154.51927	–19.7 ± 1.1
8154.56530	–24.0 ± 1.1
8158.50489	–25.9 ± 1.1
8161.43027	+21.1 ± 1.1
8162.37449	–24.7 ± 1.1
8163.53019	–34.0 ± 1.1
8164.50423	+14.0 ± 1.1
8166.57512	–39.2 ± 1.1
8168.32079	+12.9 ± 1.1
8168.44797	+18.0 ± 1.1
8170.42659	–37.0 ± 1.1
8170.56073	–39.8 ± 1.1
8171.38046	–31.7 ± 1.1
8171.54108	–24.7 ± 1.1
8172.48056	+21.5 ± 1.1
8173.33911	+12.1 ± 1.1
8174.33208	–38.2 ± 1.1
8174.49104	–42.1 ± 1.1
8175.35661	–27.1 ± 1.1
8175.52627	–18.9 ± 1.1
8176.40893	+21.5 ± 1.1
8177.31105	+7.5 ± 1.1
8177.42488	+2.3 ± 1.1
8178.34185	–42.4 ± 1.1
8178.42082	–43.2 ± 1.1
8179.38634	–19.0 ± 1.1
8179.56806	–9.9 ± 1.1
8183.35664	–14.5 ± 1.1
8190.42398	–42.6 ± 1.1
8197.29127	–22.6 ± 1.1
8202.30717	–37.3 ± 1.1
8202.46439	–32.1 ± 1.1
8213.42304	–43.2 ± 1.1
8214.44174	–14.8 ± 1.1
8215.28578	+23.7 ± 1.1
8216.39092	–5.8 ± 1.1
8217.28049	–43.4 ± 1.1
8218.33471	–14.1 ± 1.1
8218.40841	–10.1 ± 1.1
8219.29530	+22.4 ± 1.1
8219.42595	+23.9 ± 1.1
8220.43200	–14.1 ± 1.1
8223.40518	+25.7 ± 1.1
8226.31235	–2.3 ± 1.1
8227.31850	+22.7 ± 1.1
8228.31137	–19.3 ± 1.1

Table A2 RV measurements of HIP 23040

Date of Obs. BJD – 2450000	RV [km/s]
7729.47686	+16.3 ± 1.1
7743.20867	–40.7 ± 1.1
7743.64393	–44.2 ± 1.1
7744.24491	–24.3 ± 1.1
7744.52109	–9.5 ± 1.1
7759.52539	–35.6 ± 1.1
7760.27312	+2.7 ± 1.1
7764.21819	+5.2 ± 1.1
7773.29456	+8.5 ± 1.1
7775.23967	–27.3 ± 1.1
7775.31930	–24.7 ± 1.1
7776.27412	+20.6 ± 1.1
7776.56061	+23.0 ± 1.1
7780.25179	+22.0 ± 1.1
7780.61282	+23.4 ± 1.1
7782.27518	–43.8 ± 1.1
7782.36730	–45.5 ± 1.1
7786.39259	–45.0 ± 1.1
7798.35257	–36.7 ± 1.1
7798.50655	–31.2 ± 1.1
7799.35985	+14.2 ± 1.1
7799.53053	+19.6 ± 1.1
7800.35056	+14.8 ± 1.1
7800.53099	+5.9 ± 1.1
7812.30577	–1.0 ± 1.1
7826.41535	+8.1 ± 1.1
7826.45006	+9.6 ± 1.1
7840.30417	–44.8 ± 1.1
7840.49964	–43.8 ± 1.1
7841.30362	–25.7 ± 1.1
7841.40664	–22.3 ± 1.1
7843.30108	+4.8 ± 1.1
7843.46655	–4.6 ± 1.1
7864.33996	–38.0 ± 1.1
7874.37330	+5.4 ± 1.1
7876.40554	–17.4 ± 1.1

Continued	
Date of Obs. BJD – 2450000	RV [km/s]
8229.35252	-40.4 ± 1.1
8230.32692	$+6.5 \pm 1.1$
8230.42533	$+10.9 \pm 1.1$
8232.41707	-31.1 ± 1.1
8236.33528	-34.4 ± 1.1
8238.33184	$+16.1 \pm 1.1$
8239.35115	$+13.3 \pm 1.1$
8240.34454	-39.6 ± 1.1
8243.31857	$+10.9 \pm 1.1$
8244.32752	-40.0 ± 1.1
8245.33033	-24.1 ± 1.1
8246.33149	$+22.3 \pm 1.1$
8247.31681	$+0.9 \pm 1.1$
8248.36928	-45.6 ± 1.1
8252.33853	-43.7 ± 1.1
8253.33877	-10.2 ± 1.1
8264.34598	-41.0 ± 1.1

Table A3 RV measurements of HIP 2225

Date of Obs. BJD – 2450000	RV ₁ [km/s]	RV ₂ [km/s]
7729.29877	$+5.6 \pm 2.3$	
7743.19728	$+41.5 \pm 2.3$	-27.8 ± 5.9
7743.42810	$+61.1 \pm 2.3$	-48.9 ± 5.9
7744.23432	$+59.8 \pm 2.3$	-45.9 ± 5.9
7760.26168	$+51.1 \pm 2.3$	-20.3 ± 5.9
7764.20643	$+50.1 \pm 2.3$	-40.3 ± 5.9
7773.27365	-11.3 ± 2.3	$+92.9 \pm 5.9$
7775.22609	$+69.3 \pm 2.3$	-57.3 ± 5.9
7775.30591	$+72.2 \pm 2.3$	-63.7 ± 5.9
7776.26072	$+37.9 \pm 2.3$	
7780.23921	$+37.0 \pm 2.3$	
7782.26301	-2.9 ± 2.3	
7782.35320	$+6.1 \pm 2.3$	
7786.38003	$+10.8 \pm 2.3$	
7798.33964	$+19.5 \pm 2.3$	
7799.34737	$+70.4 \pm 2.3$	-54.2 ± 5.9
7800.33869	$+19.8 \pm 2.3$	
8146.26468	-1.6 ± 2.3	
8149.25184	-28.1 ± 2.3	$+91.4 \pm 5.9$
8149.37150	-31.4 ± 2.3	$+102.5 \pm 5.9$
8151.33825	$+62.5 \pm 2.3$	-70.6 ± 5.9
8155.24540	$+63.1 \pm 2.3$	-70.2 ± 5.9
8162.36250	$+21.0 \pm 2.3$	
8166.22019	$+13.5 \pm 2.3$	
8168.30229	$+5.5 \pm 2.3$	
8173.25304	-33.8 ± 2.3	$+93.0 \pm 5.9$
8174.23479	$+20.6 \pm 2.3$	

Continued		
Date of Obs. BJD – 2450000	RV ₁ [km/s]	RV ₂ [km/s]
8175.26104	$+56.5 \pm 2.3$	-50.7 ± 5.9
8178.25545	$+28.6 \pm 2.3$	
8179.30977	$+51.7 \pm 2.3$	-57.1 ± 5.9
8183.31206	$+50.8 \pm 2.3$	-57.0 ± 5.9
8197.26890	-32.7 ± 2.3	$+86.1 \pm 5.9$
8202.28991	$+54.3 \pm 2.3$	-56.7 ± 5.9
8269.51271	$+54.9 \pm 2.3$	-64.7 ± 5.9
8272.52835	-27.7 ± 2.3	$+83.9 \pm 5.9$
8273.54855	$+56.0 \pm 2.3$	-71.2 ± 5.9

Table A4 RV measurements of HIP 30247

Date of Obs. BJD – 2450000	RV [km/s]
7729.48413	-26.4 ± 0.8
7743.21598	-29.5 ± 0.8
7743.65114	-22.8 ± 0.8
7744.25195	-8.4 ± 0.8
7744.52804	-0.0 ± 0.8
7759.59163	$+32.3 \pm 0.8$
7760.29840	$+17.6 \pm 0.8$
7764.22588	$+7.5 \pm 0.8$
7773.33327	$+16.4 \pm 0.8$
7775.24820	-29.9 ± 0.8
7775.32734	-30.1 ± 0.8
7776.28259	-20.3 ± 0.8
7776.56980	-12.8 ± 0.8
7780.26028	$+4.0 \pm 0.8$
7780.60512	-7.0 ± 0.8
7786.40730	$+14.7 \pm 0.8$
7798.36956	$+34.0 \pm 0.8$
7798.51495	$+34.2 \pm 0.8$
7799.37443	$+16.1 \pm 0.8$
7799.53873	$+11.6 \pm 0.8$
7800.36601	-13.8 ± 0.8
7800.53927	-19.0 ± 0.8
7812.32202	$+18.1 \pm 0.8$
7812.33992	$+17.6 \pm 0.8$
7826.38538	-12.7 ± 0.8
7826.45871	-15.3 ± 0.8
7840.29120	-28.6 ± 0.8
7840.50940	-30.3 ± 0.8
7841.28789	-20.0 ± 0.8
7841.41769	-16.1 ± 0.8
7843.35911	$+32.5 \pm 0.8$
7843.47680	$+33.1 \pm 0.8$
7864.35739	$+15.9 \pm 0.8$
7874.38269	-6.5 ± 0.8
7874.47676	-3.5 ± 0.8

Continued	
Date of Obs. BJD – 2450000	RV [km/s]
7876.41930	+34.2 ± 0.8
7880.38713	–18.9 ± 0.8
8146.32840	–28.5 ± 0.8
8149.33891	+34.7 ± 0.8
8149.43473	+33.2 ± 0.8
8151.43858	–14.6 ± 0.8
8151.60186	–19.2 ± 0.8
8154.46383	+12.0 ± 0.8
8154.52869	+13.6 ± 0.8
8154.57471	+15.4 ± 0.8
8155.39213	+32.3 ± 0.8
8158.52164	–26.8 ± 0.8
8161.44858	+25.1 ± 0.8
8162.43935	+34.0 ± 0.8
8163.55380	+11.7 ± 0.8
8164.54241	–16.7 ± 0.8
8166.56272	–13.9 ± 0.8
8168.35845	+31.9 ± 0.8
8168.45663	+31.7 ± 0.8
8170.45984	–0.4 ± 0.8
8170.57111	–3.8 ± 0.8
8171.41264	–24.2 ± 0.8
8171.55471	–27.0 ± 0.8
8172.49136	–27.9 ± 0.8
8173.51753	–2.0 ± 0.8
8173.58668	–1.0 ± 0.8
8174.34104	+22.7 ± 0.8
8174.50037	+26.1 ± 0.8
8175.36652	+34.0 ± 0.8
8176.41855	+15.7 ± 0.8
8176.60954	+10.4 ± 0.8
8177.32806	–11.2 ± 0.8
8177.43395	–13.0 ± 0.8
8178.36580	–29.2 ± 0.8
8178.46354	–30.2 ± 0.8
8179.50388	–17.1 ± 0.8
8179.57736	–15.8 ± 0.8
8183.36692	+2.3 ± 0.8
8190.43306	–14.3 ± 0.8
8197.30045	–23.0 ± 0.8
8202.31573	+20.3 ± 0.8
8202.47888	+15.6 ± 0.8
8213.44009	+24.1 ± 0.8
8214.46228	+33.3 ± 0.8
8215.34231	+18.9 ± 0.8
8216.41457	–13.4 ± 0.8
8217.28883	–29.6 ± 0.8
8218.34449	–22.0 ± 0.8
8218.41760	–18.7 ± 0.8
8219.37338	+7.7 ± 0.8
8219.43695	+9.9 ± 0.8

Continued	
Date of Obs. BJD – 2450000	RV [km/s]
8223.41433	–24.1 ± 0.8
8226.32107	+21.8 ± 0.8
8227.37119	+34.9 ± 0.8
8228.32089	+20.6 ± 0.8
8229.36233	–12.8 ± 0.8
8230.33596	–30.0 ± 0.8
8230.41585	–29.9 ± 0.8
8232.40959	+9.1 ± 0.8
8236.34385	–25.0 ± 0.8
8238.35157	–7.3 ± 0.8
8239.37004	+23.3 ± 0.8
8240.36838	+34.1 ± 0.8
8243.33674	–29.5 ± 0.8
8244.34366	–20.4 ± 0.8
8245.34581	+8.1 ± 0.8
8246.34864	+31.1 ± 0.8
8247.32548	+28.4 ± 0.8
8248.37805	+3.4 ± 0.8
8252.34703	+20.1 ± 0.8
8253.34657	+34.0 ± 0.8
8259.33691	+30.6 ± 0.8
8260.33902	+28.5 ± 0.8
8264.35463	–6.5 ± 0.8
8265.35050	+21.7 ± 0.8
8267.35086	+16.0 ± 0.8

Table A5 RV measurements of HIP 113048

Date of Obs. BJD – 2450000	RV [km/s]
7728.36223	+2.6 ± 0.6
7729.30555	+2.1 ± 0.6
7743.27670	+10.6 ± 0.6
7744.22614	+10.9 ± 0.6
7760.25264	+7.2 ± 0.6
7764.28884	+9.3 ± 0.6
7773.26485	+6.4 ± 0.6
7775.28751	+3.2 ± 0.6
7776.25211	+2.1 ± 0.6
7798.29252	+4.5 ± 0.6
7800.29643	+3.1 ± 0.6
7840.60435	+10.6 ± 0.6
7843.62216	+12.0 ± 0.6
7874.50114	+2.9 ± 0.6
8151.24325	+9.4 ± 0.6
8155.31430	+11.8 ± 0.6
8174.24593	+7.7 ± 0.6
8175.24795	+7.6 ± 0.6
8197.66505	+7.7 ± 0.6
8202.63997	+11.7 ± 0.6

Continued		Continued	
Date of Obs.	RV	Date of Obs.	RV
BJD – 2450000	[km/s]	BJD – 2450000	[km/s]
8207.61953	+8.6 ± 0.6	8146.30295	+12.5 ± 2.8
8215.62892	+2.9 ± 0.6	8149.27496	–6.6 ± 2.8
8216.64021	+4.9 ± 0.6	8151.43120	–12.6 ± 2.8
8217.63502	+6.0 ± 0.6	8154.47172	–16.0 ± 2.8
8218.62702	+5.7 ± 0.6	8158.51362	–10.5 ± 2.8
8219.60784	+6.9 ± 0.6	8161.44113	–0.8 ± 2.8
8220.62113	+7.7 ± 0.6	8162.41505	+12.7 ± 2.8
8228.63059	+11.6 ± 0.6	8163.54639	+14.7 ± 2.8
8229.61740	+10.3 ± 0.6	8164.53386	+21.6 ± 2.8
8230.59348	+10.6 ± 0.6	8166.54872	+32.0 ± 2.8
8238.59246	+1.9 ± 0.6	8168.34173	+45.2 ± 2.8
8240.47772	+3.6 ± 0.6	8170.43537	+54.0 ± 2.8
8243.49387	+5.9 ± 0.6	8171.40315	+59.2 ± 2.8
8244.48957	+6.9 ± 0.6	8172.49950	+55.8 ± 2.8
8245.45214	+7.0 ± 0.6	8173.52487	+54.3 ± 2.8
8246.50147	+7.6 ± 0.6	8174.48287	+56.7 ± 2.8
8264.42488	+3.2 ± 0.6	8175.37457	+43.4 ± 2.8
8265.47786	+3.8 ± 0.6	8176.46248	+40.2 ± 2.8
8267.47378	+5.6 ± 0.6	8177.31903	+40.7 ± 2.8
8269.41918	+6.4 ± 0.6	8179.35163	+25.7 ± 2.8
8272.43316	+9.3 ± 0.6	8183.37853	–2.3 ± 2.8
8273.41615	+9.5 ± 0.6	8190.43942	–16.2 ± 2.8
		8197.41341	+12.2 ± 2.8
		8202.34623	+44.2 ± 2.8
		8207.41584	+56.6 ± 2.8
		8213.43115	+27.2 ± 2.8
		8214.45061	+20.7 ± 2.8
		8215.29403	+10.8 ± 2.8
		8216.40131	+7.4 ± 2.8
		8217.32291	+1.9 ± 2.8
		8218.39959	–5.5 ± 2.8
		8219.36300	–12.2 ± 2.8
		8226.32948	–12.2 ± 2.8
		8227.32661	–11.3 ± 2.8
		8228.34543	–8.0 ± 2.8
		8229.37011	–5.0 ± 2.8
		8230.34292	–1.3 ± 2.8
		8236.35027	+32.5 ± 2.8
		8238.34104	+46.9 ± 2.8
		8240.35399	+46.2 ± 2.8
		8243.32639	+50.8 ± 2.8
		8244.33485	+48.9 ± 2.8
		8245.33729	+37.9 ± 2.8
		8246.33954	+35.8 ± 2.8
		8252.32785	+2.3 ± 2.8
		8253.32727	–4.2 ± 2.8

Table A6 RV measurements of HIP 25048

Date of Obs.	RV
BJD – 2450000	[km/s]
7728.39985	+38.9 ± 2.8
7729.50042	+29.0 ± 2.8
7744.23421	–17.2 ± 2.8
7744.50516	–8.8 ± 2.8
7759.58410	+53.2 ± 2.8
7760.28077	+53.2 ± 2.8
7764.24484	+35.3 ± 2.8
7773.32607	–16.6 ± 2.8
7775.26858	–22.3 ± 2.8
7776.59037	–15.0 ± 2.8
7780.26722	–3.0 ± 2.8
7782.28313	+5.3 ± 2.8
7786.40001	+25.8 ± 2.8
7798.36115	+32.3 ± 2.8
7799.36708	+22.8 ± 2.8
7800.35821	+20.1 ± 2.8
7812.31385	–12.1 ± 2.8
7826.42281	+50.9 ± 2.8
7840.29714	–8.0 ± 2.8
7841.29693	–17.5 ± 2.8
7843.35039	–13.6 ± 2.8
7849.42947	–2.7 ± 2.8
7864.34770	+50.3 ± 2.8

Table A7 RV measurements of HIP 85829

Date of Obs. BJD – 2450000	RV [km/s]
7728.28416	-22.8 ± 0.8
7729.21441	-23.5 ± 0.8
7743.23837	-21.2 ± 0.8
7744.18086	-20.7 ± 0.8
7759.60248	-11.1 ± 0.8
7760.19004	-12.0 ± 0.8
7764.24887	-19.8 ± 0.8
7773.62955	-27.0 ± 0.8
7775.57755	-28.3 ± 0.8
7776.59693	-26.2 ± 0.8
7780.57779	-23.6 ± 0.8
7782.59454	-19.7 ± 0.8
7798.67166	-13.3 ± 0.8
7799.65676	-15.0 ± 0.8
7800.65083	-16.6 ± 0.8
7826.44009	-7.9 ± 0.8
7840.38590	-19.2 ± 0.8
7841.34600	-21.9 ± 0.8
7843.38080	-24.2 ± 0.8
7864.37753	-8.0 ± 0.8
7874.36547	-11.6 ± 0.8
7876.39810	-15.1 ± 0.8
7880.38006	-21.7 ± 0.8
8151.62384	-26.6 ± 0.8
8154.54982	-28.0 ± 0.8
8155.63042	-24.6 ± 0.8
8158.71864	-23.7 ± 0.8
8163.57372	-16.9 ± 0.8
8164.59799	-15.4 ± 0.8
8166.52981	-12.2 ± 0.8
8166.62025	-12.1 ± 0.8
8170.48567	-5.8 ± 0.8
8171.48526	-5.3 ± 0.8
8172.54915	-4.9 ± 0.8
8173.55009	-5.4 ± 0.8
8174.63598	-5.4 ± 0.8
8177.51064	-9.4 ± 0.8
8178.50990	-11.3 ± 0.8
8179.52909	-13.2 ± 0.8
8190.48728	-25.5 ± 0.8
8197.47083	-23.4 ± 0.8
8202.49429	-15.1 ± 0.8
8207.63888	-7.7 ± 0.8
8213.50249	-7.5 ± 0.8
8214.63780	-8.6 ± 0.8
8215.52753	-9.2 ± 0.8
8216.58140	-11.7 ± 0.8

Continued

Date of Obs. BJD – 2450000	RV [km/s]
8217.58282	-14.8 ± 0.8
8218.43050	-15.3 ± 0.8
8219.41335	-16.7 ± 0.8
8220.49339	-17.5 ± 0.8
8223.45411	-23.6 ± 0.8
8226.39979	-24.0 ± 0.8
8227.41248	-25.1 ± 0.8
8228.39390	-26.4 ± 0.8
8229.39840	-27.2 ± 0.8
8230.35739	-26.7 ± 0.8
8232.36948	-26.6 ± 0.8
8236.53855	-24.4 ± 0.8
8238.39563	-20.9 ± 0.8
8239.44895	-17.6 ± 0.8
8240.40113	-18.3 ± 0.8
8243.38329	-12.3 ± 0.8
8244.38503	-11.0 ± 0.8
8245.38966	-7.1 ± 0.8
8246.40243	-5.9 ± 0.8
8248.42605	-5.3 ± 0.8
8252.39887	-8.4 ± 0.8
8256.39567	-14.4 ± 0.8
8259.37366	-19.9 ± 0.8
8260.37372	-21.1 ± 0.8
8264.40299	-24.0 ± 0.8
8265.39885	-26.1 ± 0.8
8267.39249	-27.5 ± 0.8
8269.38291	-26.4 ± 0.8
8272.38151	-26.8 ± 0.8
8273.36242	-24.3 ± 0.8

Table A8 RV measurements of HIP 77986

Date of Obs. BJD – 2450000	RV [km/s]
7728.72170	-12.5 ± 2.6
7743.65296	-20.1 ± 2.6
7744.65014	-17.0 ± 2.6
7759.59463	-29.9 ± 2.6
7773.62136	-13.4 ± 2.6
7775.56958	-9.8 ± 2.6
7776.57561	-9.0 ± 2.6
7780.57046	-7.7 ± 2.6
7782.58725	-12.4 ± 2.6
7798.66521	-19.3 ± 2.6
7799.65017	-23.8 ± 2.6
7800.64464	-24.3 ± 2.6
7826.43460	-12.2 ± 2.6
7840.38068	-16.5 ± 2.6
7843.37367	-17.1 ± 2.6

Continued		Date of Obs.	RV
Date of Obs.	RV	BJD – 2450000	[km/s]
BJD – 2450000	[km/s]		
7849.45919	-22.8 ± 2.6	7728.33086	-54.6 ± 2.0
7864.37104	-11.7 ± 2.6	7729.26383	-58.0 ± 2.0
7870.38671	-9.1 ± 2.6	7743.24548	+24.4 ± 2.0
7874.35860	-11.8 ± 2.6	7744.18793	+28.6 ± 2.0
7876.38293	-13.3 ± 2.6	7760.19605	+2.0 ± 2.0
7880.37228	-12.1 ± 2.6	7764.25453	-7.3 ± 2.0
8151.61362	-15.1 ± 2.6	7773.19967	-30.7 ± 2.0
8155.61993	-17.3 ± 2.6	7776.20761	-34.0 ± 2.0
8158.64372	-21.5 ± 2.6	7780.21947	-43.7 ± 2.0
8163.56405	-21.6 ± 2.6	7782.21305	-43.1 ± 2.0
8164.58841	-24.5 ± 2.6	7798.67700	-60.4 ± 2.0
8166.51779	-21.4 ± 2.6	7799.66201	-58.2 ± 2.0
8170.47201	-29.5 ± 2.6	7800.66233	-56.5 ± 2.0
8171.49803	-27.4 ± 2.6	7840.51943	-22.2 ± 2.0
8172.53880	-26.9 ± 2.6	7841.51707	-23.3 ± 2.0
8173.53814	-24.0 ± 2.6	7843.51749	-28.4 ± 2.0
8174.62605	-26.7 ± 2.6	7849.53985	-38.7 ± 2.0
8177.49942	-24.9 ± 2.6	7874.42166	-45.8 ± 2.0
8178.49972	-25.8 ± 2.6	7876.46334	-34.9 ± 2.0
8179.51861	-24.0 ± 2.6	7880.49384	+0.8 ± 2.0
8190.45404	-12.7 ± 2.6	8151.72436	-56.2 ± 2.0
8197.46118	-16.0 ± 2.6	8155.71629	-43.1 ± 2.0
8202.40438	-15.4 ± 2.6	8163.72153	+20.2 ± 2.0
8213.45481	-24.8 ± 2.6	8171.62854	+31.5 ± 2.0
8214.58007	-24.5 ± 2.6	8172.60912	+25.5 ± 2.0
8215.51849	-24.7 ± 2.6	8173.62579	+25.0 ± 2.0
8216.57255	-26.0 ± 2.6	8174.64352	+22.1 ± 2.0
8217.57393	-24.9 ± 2.6	8177.62698	+13.1 ± 2.0
8218.44600	-30.7 ± 2.6	8178.64245	+11.7 ± 2.0
8219.40032	-34.6 ± 2.6	8179.64848	+4.5 ± 2.0
8220.48412	-27.0 ± 2.6	8197.60999	-33.8 ± 2.0
8223.43087	-24.9 ± 2.6	8202.53485	-42.4 ± 2.0
8226.39099	-25.0 ± 2.6	8207.53309	-52.7 ± 2.0
8227.40056	-23.5 ± 2.6	8213.57149	-59.9 ± 2.0
8228.37578	-19.2 ± 2.6	8215.53530	-62.9 ± 2.0
8229.38866	-24.1 ± 2.6	8216.58840	-62.0 ± 2.0
8230.36857	-16.7 ± 2.6	8217.58957	-65.3 ± 2.0
8232.38070	-19.1 ± 2.6	8220.50220	-62.9 ± 2.0
8236.52674	-14.9 ± 2.6	8223.46652	-60.3 ± 2.0
8238.38652	-16.8 ± 2.6	8227.52998	-31.5 ± 2.0
8243.37388	-12.9 ± 2.6	8228.53513	-26.7 ± 2.0
8244.37613	-13.7 ± 2.6	8229.52736	-15.8 ± 2.0
8245.38068	-17.8 ± 2.6	8230.46303	-10.4 ± 2.0
8246.39029	-17.0 ± 2.6	8236.54768	+30.7 ± 2.0
8252.38993	-20.0 ± 2.6	8240.49987	+31.5 ± 2.0
8258.37459	-26.0 ± 2.6	8243.43850	+26.7 ± 2.0
8259.36406	-28.9 ± 2.6	8245.44952	+21.6 ± 2.0
8264.39321	-29.7 ± 2.6	8246.45394	+14.4 ± 2.0
		8248.59410	+11.2 ± 2.0

Table A9 RV measurements of HIP 98194

Continued	
Date of Obs. BJD – 2450000	RV [km/s]
8252.40786	+1.9 ± 2.0
8256.40448	–11.3 ± 2.0
8259.38326	–13.5 ± 2.0
8260.38323	–16.9 ± 2.0
8264.41324	–30.2 ± 2.0
8265.41290	–26.8 ± 2.0
8267.40148	–34.9 ± 2.0
8269.39227	–41.5 ± 2.0
8272.41428	–45.0 ± 2.0
8273.39399	–45.8 ± 2.0

Table A10 RV measurements of HIP 107136

Date of Obs. BJD – 2450000	RV [km/s]
7728.34768	+0.8 ± 3.1
7729.27877	–1.2 ± 3.1
7743.25461	–5.6 ± 3.1
7744.21207	–0.6 ± 3.1
7760.23788	–5.6 ± 3.1
7764.26354	–2.5 ± 3.1
7773.21582	–7.1 ± 3.1
7775.27287	–4.7 ± 3.1
7776.23554	–5.9 ± 3.1
7782.23981	–3.4 ± 3.1
7798.27627	+0.7 ± 3.1
7799.28929	–2.8 ± 3.1
7800.25683	–3.2 ± 3.1
7840.52799	–9.2 ± 3.1
7841.52315	–7.7 ± 3.1
7843.60106	–0.5 ± 3.1
7874.45321	–4.4 ± 3.1
7880.44362	–1.5 ± 3.1
8146.24573	–8.2 ± 3.1
8151.22587	–7.6 ± 3.1
8155.29609	–6.7 ± 3.1
8162.31356	–9.0 ± 3.1
8171.66083	–6.7 ± 3.1
8172.65879	–4.7 ± 3.1
8173.64684	–5.6 ± 3.1
8174.68695	–2.1 ± 3.1
8176.63254	–3.6 ± 3.1
8178.65356	–5.1 ± 3.1
8197.62064	–7.7 ± 3.1
8202.57024	–2.5 ± 3.1
8207.54446	–6.3 ± 3.1
8214.64218	–8.0 ± 3.1
8215.60049	–5.2 ± 3.1
8216.65166	–6.3 ± 3.1

Continued	
Date of Obs. BJD – 2450000	RV [km/s]
8217.64715	–7.7 ± 3.1
8219.57666	–10.6 ± 3.1
8220.59183	–10.6 ± 3.1
8228.59445	–7.8 ± 3.1
8229.59686	–10.6 ± 3.1
8230.56516	–11.1 ± 3.1
8232.55260	–4.9 ± 3.1
8238.46692	–9.6 ± 3.1
8240.53233	–9.5 ± 3.1
8243.52378	–3.8 ± 3.1
8244.52652	–7.7 ± 3.1
8245.50747	–3.0 ± 3.1
8246.51472	–5.3 ± 3.1
8252.58164	–6.7 ± 3.1
8256.41395	–3.3 ± 3.1
8264.47936	–8.4 ± 3.1
8265.48615	–5.4 ± 3.1
8267.48187	–7.9 ± 3.1
8269.47253	–10.2 ± 3.1
8272.47911	–4.4 ± 3.1
8273.42054	–11.7 ± 3.1

Table A11 RV measurements of HIP 107533

Date of Obs. BJD – 2450000	RV [km/s]
7728.35402	–16.6 ± 1.2
7729.28583	–15.4 ± 1.2
7743.26866	–16.9 ± 1.2
7744.21863	–16.2 ± 1.2
7760.28400	–17.4 ± 1.2
7764.28035	–16.7 ± 1.2
7773.23083	–15.7 ± 1.2
7775.27993	–16.8 ± 1.2
7776.24328	–16.8 ± 1.2
7782.24702	–17.7 ± 1.2
7798.28327	–16.5 ± 1.2
7799.29815	–17.5 ± 1.2
7800.24873	–16.6 ± 1.2
7840.53464	–15.8 ± 1.2
7841.52975	–14.4 ± 1.2
7843.61561	–17.4 ± 1.2
7874.46144	–17.1 ± 1.2
7880.45123	–15.7 ± 1.2
8146.25345	–16.4 ± 1.2
8151.23414	–18.9 ± 1.2
8155.30427	–17.4 ± 1.2
8162.32888	–16.5 ± 1.2
8171.66904	–17.0 ± 1.2
8172.66630	–16.8 ± 1.2

Continued

Date of Obs. BJD – 2450000	RV [km/s]
8173.66925	-18.0 ± 1.2
8174.70697	-18.2 ± 1.2
8176.63996	-18.2 ± 1.2
8178.66027	-17.4 ± 1.2
8179.63646	-17.6 ± 1.2
8197.62828	-18.0 ± 1.2
8202.58052	-18.6 ± 1.2
8207.57900	-17.9 ± 1.2
8215.62021	-16.7 ± 1.2
8216.65828	-16.5 ± 1.2
8217.65830	-16.6 ± 1.2
8219.59906	-16.5 ± 1.2
8220.61231	-18.4 ± 1.2
8228.62179	-17.9 ± 1.2
8230.58527	-18.2 ± 1.2
8238.47419	-15.7 ± 1.2
8240.55271	-16.0 ± 1.2
8243.54366	-16.7 ± 1.2
8244.54650	-18.9 ± 1.2
8245.52753	-17.2 ± 1.2
8246.59662	-18.4 ± 1.2
8252.58853	-15.9 ± 1.2
8264.50000	-18.3 ± 1.2
8265.55263	-16.2 ± 1.2
8267.50238	-19.4 ± 1.2
8269.49318	-18.7 ± 1.2
8272.50371	-20.4 ± 1.2
8273.49114	-19.5 ± 1.2